J Mater Sci (2018) 53:2171–2180

Metals

Size-dependent surface thermodynamic properties of nano-copper and its determination method by equilibrium constant

Zongru Li[1], Qingshan Fu[1], Yongqiang Xue[1,*], and Zixiang Cui[1]

[1] *Department of Applied Chemistry, Taiyuan University of Technology, Taiyuan 030024, People's Republic of China*

Received: 27 May 2017
Accepted: 26 September 2017

ABSTRACT

The surface thermodynamic properties play an important role in researching into the thermodynamics of nanoparticles involved in various chemical and physical processes. In this paper, the relations between surface thermodynamics properties, respectively, and particle size of nanoparticles were deduced. A new method of determining the surface thermodynamic properties of nano-copper by equilibrium constant was proposed. On the basis of the equilibrium constants of nano-copper with different particle sizes dissolved in sulfuric acid at different temperatures, the effect of particle size on the surface thermodynamic properties was investigated and the variation of surface tension with temperature was obtained. The influence regularities of size on the surface thermodynamic properties agree with the theoretical analysis. With the decrease in particle size, the molar surface Gibbs energy, the molar surface enthalpy and the molar surface entropy increase, and when the diameter exceeds 20 nm, the surface thermodynamic properties exhibit linear correlation with the reciprocal of diameter, respectively. The surface tension decreases with temperature increasing, and a linear relation between them is observed. This paper provides us a simple and reliable method to obtain the surface thermodynamic properties of nanoparticles for better understanding their thermodynamic behaviors in the chemical reaction, adsorption, melting, etc.

Introduction

Nano-materials have received steadily growing concern owing to their important role as a bridge between atoms and bulk materials, as well as their peculiar properties and widespread applications ranging from adsorption [1] to phase transition [2, 3], dissolution [4–6], electrochemical [7–9], some other fundamental researches [10, 11], etc, while almost all of the particular properties of nano-materials are influenced by the surface thermodynamics [12] which depend on the size of nanoparticles constitute the nano-materials. So it would be benefit for all studies and applications of nano-materials to investigate the

---

Address correspondence to E-mail: xyqlw@126.com

DOI 10.1007/s10853-017-1646-9

effect of particle size on the surface thermodynamic properties.

Surface thermodynamics of nanoparticles has attracted many researchers' attention. Mazeina et al. [13] and Bomatímiguel et al. [14] obtained the surface enthalpies of nano-Akaganeite, β-FeOOH and maghemite by a series of calorimetric measurements. Huang et al. [15, 16] studied the molar surface enthalpy of Cu_2O and Ag_3PO_4 also by microcalorimetry. Zhang et al. [17] and Wang et al. [18] got the surface thermodynamic properties of nano-vaterite by the determination of the equilibrium conductivity and those of nano-Ag_2O by the method of electrochemistry, respectively. Compared with the aforementioned method of calorimetric measurements, the chemical methods possess the advantages in accuracy and convenience to determine the surface thermodynamic properties of nanoparticles. Nevertheless, the method of Zhang et al. may be limited to the insoluble salts, while that of Wang et al. is only suitable for electrode reaction.

As one of the most important parameters of the surface thermodynamic properties, the surface tension is also of interest in the behavior of nano-sized working elements. However, the solid surface tension is difficult to be determined directly, and theoretical methods have been developed to calculate or simulate the surface tension [19–23]. It is found that the effect of particle size on surface tension can be neglected when the diameter of nanoparticles approaches or exceeds 20 nm [2, 24, 25]. Sdobnyakov et al. [21] showed that the surface tension decreases with the temperature increase. When considering the size-dependent thermodynamic properties of nanomaterials, surface stress cannot be ignored [26–29], and for reversible chemical processes of nano-systems, the surface stress equals to the surface tension [30].

Herein a method to investigate the surface thermodynamics by chemical reaction was put forward. The relations of surface thermodynamic properties to particle size were derived. Then nano-Cu was taken as an example, and the effect of size on the surface thermodynamic properties was investigated by measuring the solubilities of nano-Cu with different particle sizes at different temperatures. Furthermore, the experimental results were compared with the theoretical analysis. Subsequently, the variation of surface tension of nano-Cu with temperature was discussed.

Theoretical

The Surface thermodynamic properties of nanoparticles

Under constant temperature and pressure, the surface Gibbs energy G^s of spherical nanoparticles can be expressed as follows,

$$G^s = A\sigma = N\pi\sigma d^2 \tag{1}$$

where the superscript s denotes the surface phase and σ, A, d and N denote the surface tension, the surface area, the diameter and the number of nanoparticles, respectively.

Then, the molar surface Gibbs energy can be obtained,

$$G_m^s = G^s/n = 6\sigma V_m/d \tag{2}$$

where n and V_m denote the amount of substance and the molar volume, respectively.

Equation (2) indicates that the molar surface Gibbs energy increases with particle size decreasing and exhibits a linear variation with the reciprocal of particle size for larger nanoparticles ($d > 20$ nm) because of the negligible effect particle size on surface tension [2, 24, 25]. Moreover, for general metallic nanoparticles, the orders of σ, M and ρ are 10^{-1}–10^{0} J m^{-2} [31, 32], 10^{-2}–10^{-1} kg mol^{-1} and 10^{3}–10^{4} kg m^{-3}, respectively. Thus, according to Eq. (2), the orders of magnitude for G_m^s are 10^{-4}–10^{-1}, 10^{-3}–10^{0} and 10^{-2}–10^{1} kJ mol^{-1}, respectively, when the orders of r are 10^{-6}, 10^{-7} and 10^{-8} m. When $r > 10^{-6}$ m, the effect of particle size on G_m^s is so small that it can be ignored in general cases, but $r < 10^{-7}$ m, the effect becomes obvious.

Then, the molar surface enthalpy and the molar surface entropy of nanoparticles can be derived as follows,

$$H_m^s = -T^2\left[\frac{\partial}{\partial T}\left(\frac{G_m^s}{T}\right)\right]_p = \frac{6V_m}{d}\left[\sigma - T\left(\frac{\partial\sigma}{\partial T}\right)_p - \frac{2T\sigma\alpha}{3}\right] \tag{3}$$

$$S_m^s = -\left(\frac{G_m^s}{T}\right)_p = -\frac{6V_m}{d}\left[\left(\frac{\partial\sigma}{\partial T}\right)_p + \frac{2\sigma\alpha}{3}\right] \tag{4}$$

where α is the coefficient of volume expansion, $\alpha = 1/V_m(\partial V_m/\partial T)_p$.

As for molten metals, the orders of magnitude of σ, T, $(\partial\sigma/\partial T)_p$ and α are 10^{0} J·m^{-2}, 10^{2} K, 10^{-4} J·m^{-2} -K^{-1} and 10^{-5} K^{-1} [33], respectively. So the value in the brackets of Eq. (3) is positive and small, and the molar surface enthalpy increases with the decrease in particle size. While for common materials, $(\partial\sigma/\partial T)_p < 0$, hence the molar surface entropy increases with particle size decreasing in terms of Eq. (4). It is obvious that there are linear relationships between the molar surface enthalpy and the molar surface entropy and the reciprocal of particle size when the diameter exceeds 20 nm.

A determination method of the surface thermodynamic properties of nano-Cu by equilibrium constant

The reaction ionic equation of nano-Cu dissolving in dilute acid is expressed as follows,

$$\mathrm{Cu}(s) + 2H^{+}(aq) \rightarrow \mathrm{Cu}^{2+}(aq) + H_2(aq) \qquad (5)$$

The molar dissolution thermodynamic properties of surface phase of nano-Cu can be derived as follows [34],

$$\Delta_{\mathrm{r}} G_{\mathrm{m}}^{\mathrm{s}} = v\mu^{\mathrm{s}} = -\frac{4\sigma V_{\mathrm{m}}}{d} \qquad (6)$$

$$\Delta_{\mathrm{r}} H_{\mathrm{m}}^{\mathrm{s}} = -\frac{4V_{\mathrm{m}}}{d}\left[\sigma - T\left(\frac{\partial\sigma}{\partial T}\right)_p - \frac{2T\sigma\alpha}{3}\right] \qquad (7)$$

$$\Delta_{\mathrm{r}} S_{\mathrm{m}}^{\mathrm{s}} = \frac{4V_{\mathrm{m}}}{d}\left[\left(\frac{\partial\sigma}{\partial T}\right)_p + \frac{2\sigma\alpha}{3}\right] \qquad (8)$$

where v and μ^{s} are the stoichiometric number and the surface chemical potential of nanoparticles, respectively.

Based on the definition of partial molar quantity, the partial molar surface Gibbs energy of nano-Cu ($G^{\mathrm{s}}_{\mathrm{Cu}}$) can be expressed as follows,

$$G^{\mathrm{s}}_{Cu} = (\partial G^{\mathrm{s}}/\partial n_{Cu})_{T,p} = 4\sigma V_m/d \qquad (9)$$

Then, the partial molar surface enthalpy $H^{\mathrm{s}}_{\mathrm{Cu}}$ and the partial molar surface entropy $S^{\mathrm{s}}_{\mathrm{Cu}}$ are obtained,

$$H^{\mathrm{s}}_{\mathrm{Cu}} = -T^2\left[\frac{\partial}{\partial T}\left(\frac{G^{\mathrm{s}}_{\mathrm{Cu}}}{T}\right)_p\right] = \frac{4V_{\mathrm{m}}}{d}\left[\sigma - T\left(\frac{\partial\sigma}{\partial T}\right)_p - \frac{2T\sigma\alpha}{3}\right] \qquad (10)$$

$$S^{\mathrm{s}}_{\mathrm{Cu}} = -\left(\frac{\partial G^{\mathrm{s}}_{\mathrm{Cu}}}{\partial T}\right)_p = -\frac{4V_{\mathrm{m}}}{d}\left[\left(\frac{\partial\sigma}{\partial T}\right)_p + \frac{2\sigma\alpha}{3}\right] \qquad (11)$$

Comparisons of Eqs. (9) and (2), (10) and (3), (11) and (4), (9) and (6), (10) and (7), (11) and (8), respectively, reveal that the ratio of the partial molar surface quantities to the corresponding molar surface quantities is 2:3, and the ratio of the partial molar surface quantities to the corresponding molar thermodynamic quantities of surface phase of nano-Cu dissolving in dilute acid is −1:1, that is,

$$M^{\mathrm{s}}_{\mathrm{m}} = (3/2)M^{\mathrm{s}}_{\mathrm{Cu}} = -(3/2)\Delta_{\mathrm{r}} M^{\mathrm{s}}_{\mathrm{m}} \qquad (12)$$

where M denotes the thermodynamic properties.

Based on the formula $\Delta G_m = -RT\ln K$, the following equation is obtained,

$$\ln\frac{K}{K^b} = -\frac{1}{RT}\Delta_{\mathrm{r}} G^s_m = -\frac{1}{RT}\frac{4v\sigma V_{\mathrm{m}}}{d} \qquad (13)$$

where K is the dissolution equilibrium constant.

It can be seen from Eq. (13) that the smaller of the particle size, the greater the equilibrium constant. And it can be deduced from Eq. (13) that the logarithm of equilibrium constant is inversely proportional to the particle size at the same temperature when the diameter of nanoparticle approaches or exceeds 20 nm.

Experimental

Preparation of nano-Cu

Spherical nano-Cu was prepared by liquid-phase reduction method [35]. Cupric sulfate was used as copper source, hydrazine hydrate diamidhydrate as reducing agent and polyvinyl pyrrolidone as dispersant. The nano-Cu with different sizes was prepared by changing the concentration of reactant and the reaction temperature. After being washed with distilled water and ethanol for several times, the obtained samples were dried at 303 K for 4 h in a vacuum oven. The detailed reaction conditions and the corresponding average particle diameters are given in Table 1.

Table 1 The average particle diameters (d) of nano-Cu prepared under different conditions

No.	T/K	pH	c($\mathrm{CuSO_4}$)/($\mathrm{mol{\cdot}L^{-1}}$)	t/h	d/nm
1.	343	11	0.5	1	21.5
2.	343	11	1.0	1	24.2
3.	323	11	0.5	1	26.2
4.	323	11	1.0	1	29.1
5.	303	11	0.5	1	35.1
6.	303	11	1.0	1	38.4

Characterization of nano-Cu

The XRD patterns of nano-Cu samples were characterized using a Germany Bruker D8 Advance Powder Diffractometer (Cu $K\alpha$, $k = 0.154178$ nm), which are shown in Fig. 1. The main characteristic peaks at 43.3°, 50.6° and 74.1° can be assigned to the (111), (200) and (220) planes of crystal structure, respectively. On the basis of the half peak width of characteristic diffraction peaks, the Scherrer formula was used to calculate the particles size of samples.

The morphology of samples was observed using JSM-6701F scanning electron microscope (SEM), which was operated at an accelerating voltage of 10.0 kV. Typical SEM images of the as-prepared nano-Cu are shown in Fig. 2. It was clear that the morphology of the as-obtained samples was nearly spherical. And Fig. 3 is the error bar on the particle sizes of nano-Cu corresponding to that of Fig. 2.

The samples were further examined with EDS, and the result is shown in Fig. 4. The EDS spectrum only exhibits the characteristic peaks of Cu, suggesting that the obtained product is composed of pure Cu.

Dissolution experiment

The reactions were performed in a beaker which was placed at a DF-101S thermostat bath with magnetic stirrer. For each reaction, 100 mg of nano-Cu with different sizes was added into 100 mL of dilute sulfuric acid (0.0500 mol L^{-1}), respectively. The pH values and the concentrations of copper ion were measured using the PXST-216 ion analysis apparatus. The values were recorded every 10 s until they are unchanged, and then, the equilibrium concentration of copper ion can be obtained. The reactions were performed at a series of temperatures, 298, 303, 308 and 313, and three parallel reactions were conducted at every temperature for minimizing experimental error.

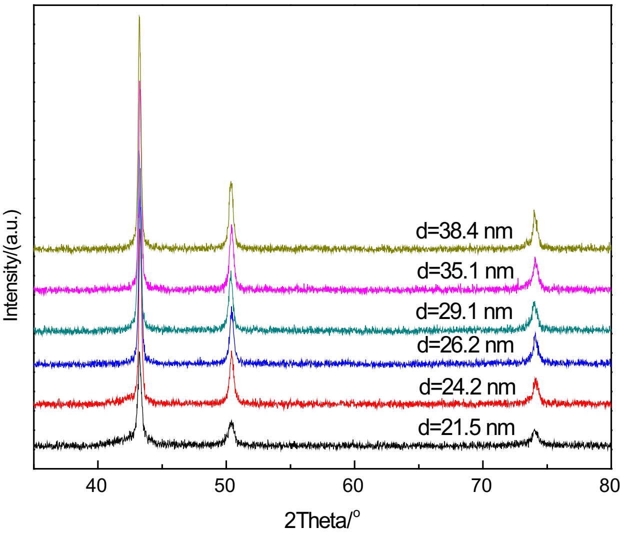

Figure 1 The XRD patterns of nano-Cu with different sizes.

Data processing

The dissolution equilibrium constant of nano-Cu in dilute acid can be obtained,

$$K = a_{Cu^{2+}} a_{\mathrm{H}_2} / a_{\mathrm{H}^+}^2 \tag{14}$$

where $a_{Cu^{2+}}$ and a_{H^+} are the activities of Cu^{2+} and H^+, respectively. The activity $a_i = \gamma_i \times c_i / c_i^o$, where c_i is ion concentration, $c_i^o = 1$ mol L^{-1}, and γ_i is the ionic activity coefficient. Especially, a_{H_2} is the activity of hydrogen molecule in the solution, and it can be seen that $a_{H_2} \approx c_{H_2}$ for the trace amounts of generated hydrogen and $\gamma_{H_2} \approx 1$. C_{H^+} can be calculated by $C_{\mathrm{Cu}^{2+}}$. Because of the high ionic strength of the solution, the activity coefficient can be estimated from the extended Debye–Hückel equation [36].

When the particle size tends to be infinite, the logarithm of equilibrium constant of the corresponding bulk copper $\ln K^b$ can be obtained. Then, the molar surface Gibbs energy of nano-Cu with different sizes can be calculated by Eq. (15),

$$G_{\mathrm{m}}^{\mathrm{s}} = -(3/2)\Delta_{\mathrm{r}} G_{\mathrm{m}}^{\mathrm{s}} = (3/2) RT \ln\left(K/K^b\right) \tag{15}$$

The surface tension of nano-Cu can be obtained by the slope of $G_{\mathrm{m}}^{\mathrm{s}}$ versus surface area. $\Delta_{\mathrm{r}} H_{\mathrm{m}}^{\mathrm{s}}$ and $\Delta_{\mathrm{r}} S_{\mathrm{m}}^{\mathrm{s}}$ can be considered as constants within the temperature ranges, and they can be calculated by the slope and the intercept of the linear regression for $\ln\left(K/K^b\right)$ on $1/T$ as Eq. (16), respectively,

$$\ln \frac{K}{K^b} = -\frac{\Delta_{\mathrm{r}} H_{\mathrm{m}}^{\mathrm{s}}}{RT} + \frac{\Delta_{\mathrm{r}} S_{\mathrm{m}}^{\mathrm{s}}}{R} \tag{16}$$

According to Eqs. (12) and (16), the molar surface entropy and the molar surface enthalpy can be also obtained,

$$H_{\mathrm{m}}^{\mathrm{s}} = -(3/2)\Delta_{\mathrm{r}} H_{\mathrm{m}}^{\mathrm{s}} \tag{17}$$

$$S_{\mathrm{m}}^{\mathrm{s}} = -(3/2)\Delta_{\mathrm{r}} S_{\mathrm{m}}^{\mathrm{s}} \tag{18}$$

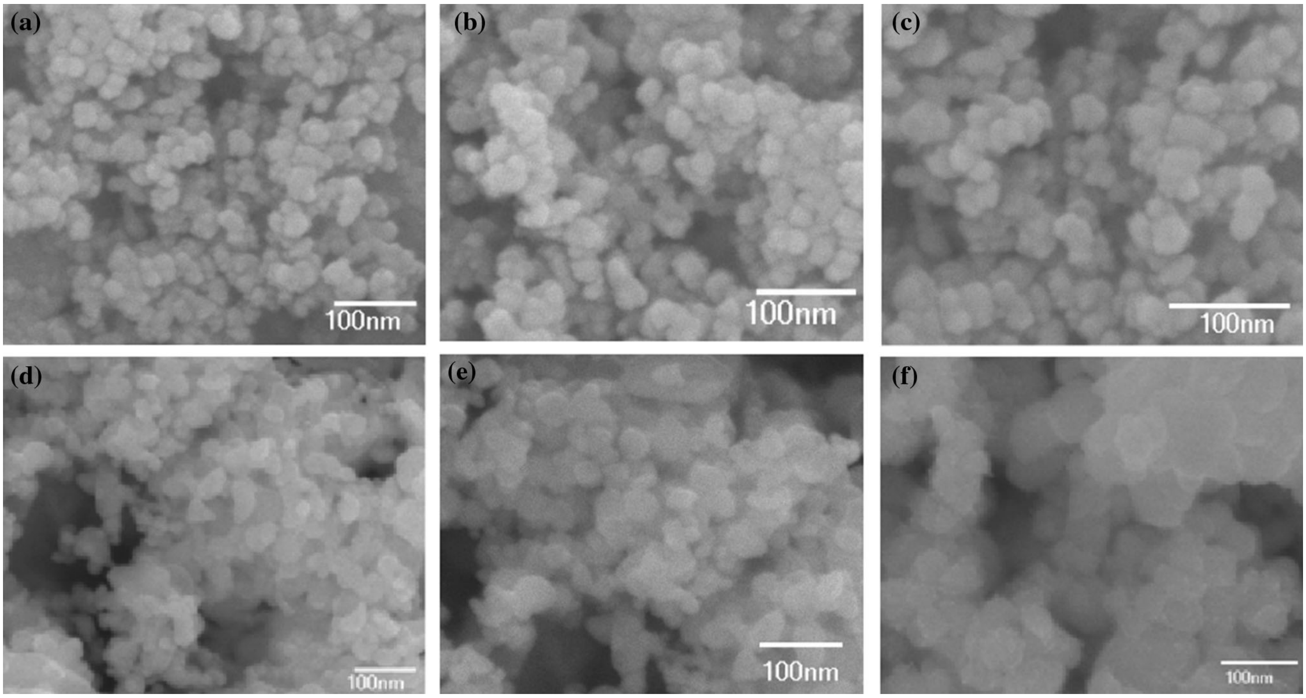

Figure 2 The SEM images of nano-Cu with different sizes, **a** 21.5 nm, **b** 24.2 nm, **c** 26.2 nm, **d** 29.1 nm, **e** 35.1 nm, **f** 38.4 nm.

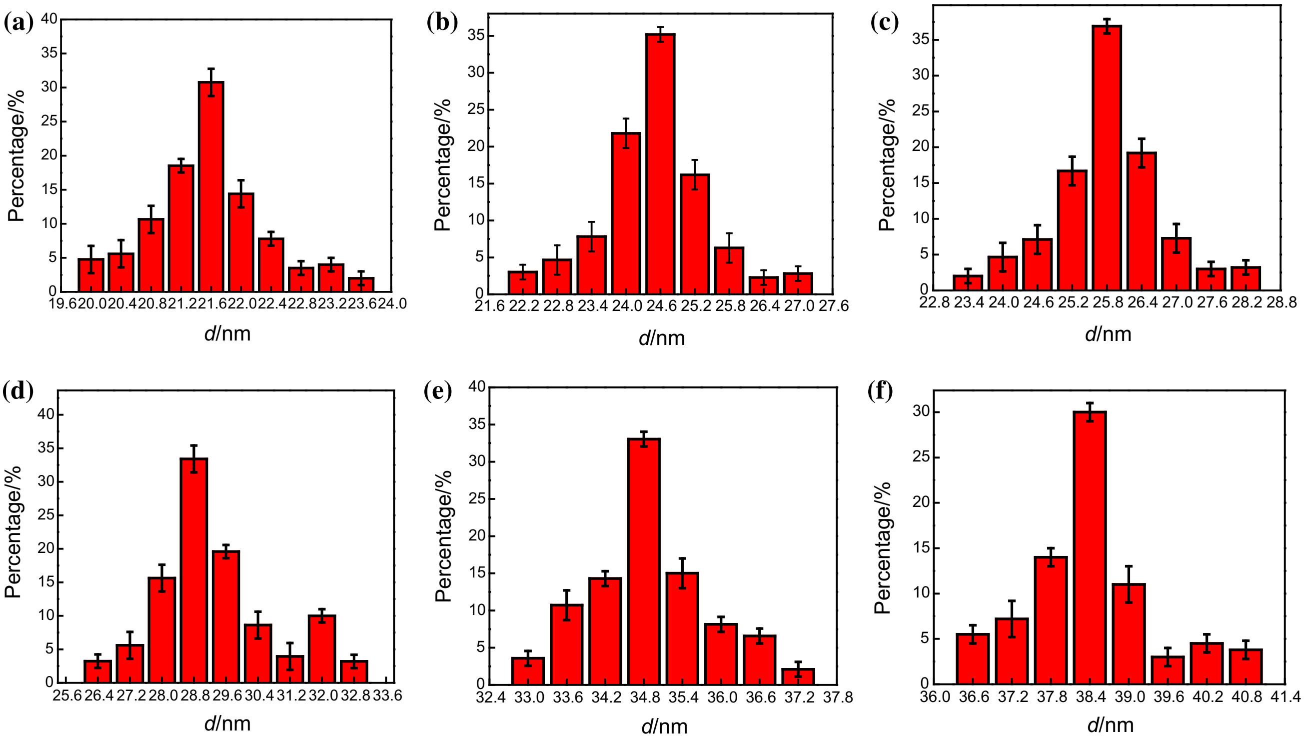

Figure 3 The error bar on the particle sizes of nano-Cu corresponding to that of Figure 2.

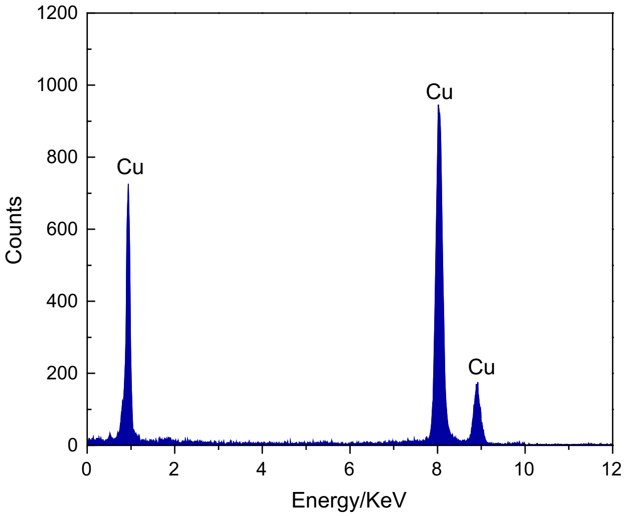

Figure 4 EDS spectrum of the nano-Cu.

Results and discussion

The activities of copper ion with different sizes at different temperatures are listed in Table 2.

It can be seen from Table 2 that the solubility of nano-Cu with the same size increases with increasing temperature; the solubility increases with decreasing particle size at a certain temperature. As the size decreases, the surface energy increases, leading to a reduction in the dissolution Gibbs energy and making it easier to dissolve.

The dissolution equilibrium constants of nano-Cu at different temperatures were calculated by Eq. (13). The effect of particle size on surface tension can be neglected when the particle diameter exceeds 20 nm, and the surface tension becomes a constant. There is a liner relationship between the logarithm of the equilibrium constant and the reciprocal of particle size, and K_b can be obtained by extrapolating of the experimental data. And then $\ln\left(K/K^b\right)$ can be calculated, and the results are shown in Table 3.

Table 3 ln (K/K^b) with different sizes at different temperatures

d/nm	d^{-1}/nm^{-1}	$\ln\left(K/K^b\right)$				
		298 K	303 K	308 K	313 K	318 K
38.4	0.0261	1.4223	1.3013	1.1979	1.1212	1.0674
35.1	0.0285	1.6576	1.4658	1.3661	1.2775	1.2040
29.1	0.0344	1.8892	1.7510	1.6432	1.5136	1.4161
26.2	0.0382	2.1151	1.9508	1.8173	1.6597	1.5319
24.2	0.0413	2.3017	2.1514	1.9935	1.8274	1.6850
21.5	0.0466	2.6177	2.3325	2.1646	2.0384	1.9503

Effect of size on the molar surface Gibbs energy of nano-Cu

We can obtain the surface Gibbs energy G_m^s of nano-Cu with different sizes at different temperatures through Eq. (15) and Table 3. The relations between G_m^s and $1/d$ are shown in Fig. 5.

Notable linear trends between G_m^s and $1/d$ are observed in Fig. 5a, and G_m^s increases as the particle size decreases, which is consistent with the theoretical analysis of Eq. (2). The orders of magnitude of G_m^s presented in Fig. 5a are in good accordance with the theoretical estimation. The results also clearly indicate that in the conditions of constant pressure and temperature, the smaller the particle size, the higher the chemical activity and the more unstable the nanoparticles. Furthermore, if these lines are extrapolated to y-axis, the value of surface Gibbs energy of nano-Cu tends to zero (see Fig. 5b). That is, the molar surface Gibbs energy of bulk materials tends to zero, which illustrates the negligible size effect on bulk materials.

Table 2 The activities of copper ion with different sizes at different temperatures

d/nm	d^{-1}/nm^{-1}	$c_{Cu^{2+}}/\text{mol}\cdot\text{L}^{-1}$				
		298 K	303 K	308 K	313 K	318 K
38.4	0.0261	2.111E−04	2.580E−04	3.097E−04	3.800E−04	4.613E−04
35.1	0.0285	2.373E−04	2.800E−04	3.367E−04	4.107E−04	4.937E−04
29.1	0.0344	2.663E−04	3.227E−04	3.863E−04	4.617E−04	5.483E−04
26.2	0.0382	2.980E−04	3.563E−04	4.212E−04	4.963E−04	5.807E−04
24.2	0.0413	3.270E−04	3.937E−04	4.597E−04	5.393E−04	6.263E−04
21.5	0.0466	3.825E−04	4.307E−04	5.003E−04	5.987E−04	7.140E−04

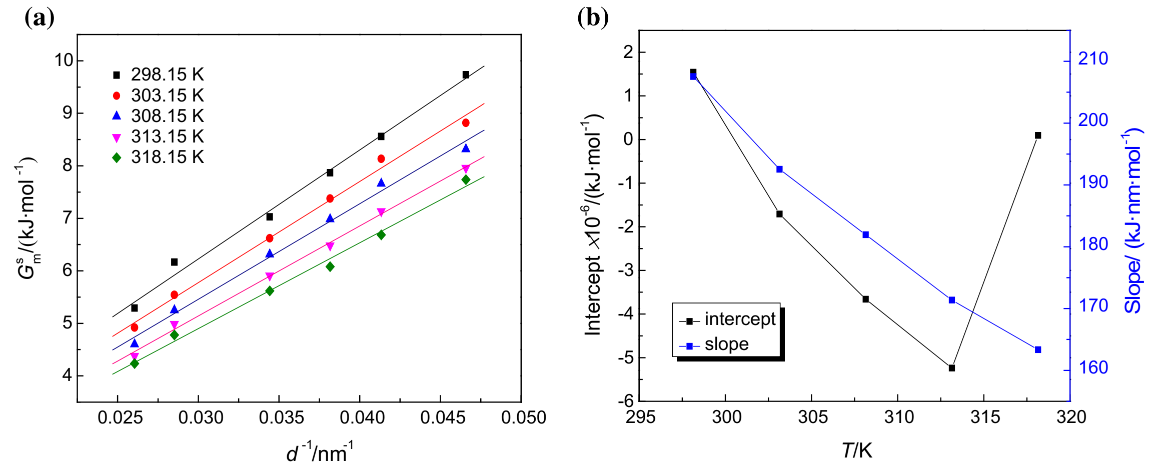

Figure 5 **a** Plot of G^s_m versus $1/d$ at different temperatures. **b** Plot of intercept (I) and slope (S) versus temperature.

Effect of temperature on surface tension of nano-Cu

Plots of the molar surface Gibbs energy versus the surface area are shown in Fig. 6.

Figure 6 shows linear relationships between G^s_m and surface area, and the slope of the line is the surface tension, which is consistent with the studies [17, 18] that the effect of particle size on surface tension can be neglected when the particle diameter exceeds 20 nm. The effect of temperature on surface tension of nano-Cu is shown in Fig. 7.

Figure 7 shows that surface tension is 3.84–4.88 J m^{-2} in the temperature range of 298–318 K. The surface tension decreases with the temperature increase, and there is a linear relationship between them. The maximal value of surface tension of liquid copper is 1.33 J m^{-2} from the melting temperature to the critical temperature [32], and the surface tension decreases with the temperature increasing [21]. The surface tension of solid is larger than that of the corresponding liquid [2], which satisfactorily accounts for the larger value of the surface tension of solid nano-copper.

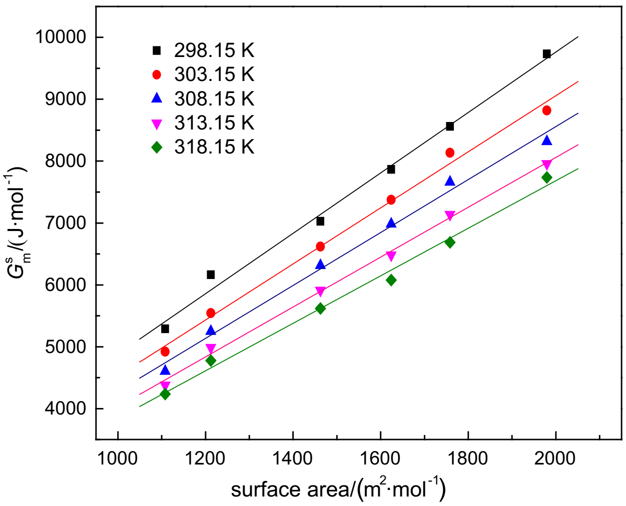

Figure 6 Plots of G^s_m versus surface area.

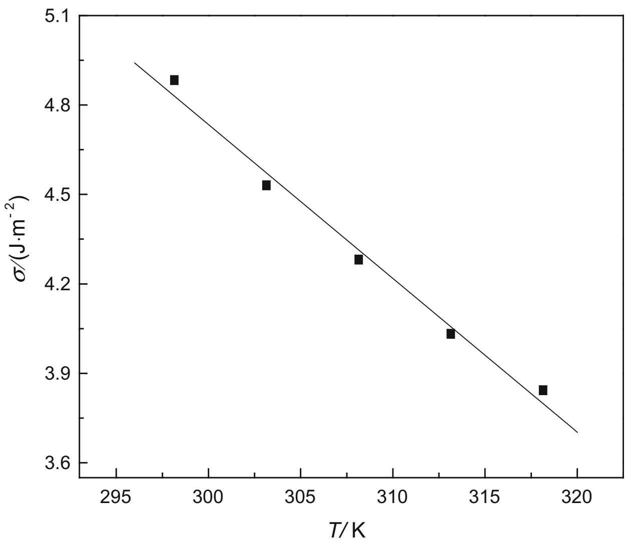

Figure 7 The relation between surface tension and temperature.

Effect of size on the molar surface enthalpy and entropy of nano-Cu

The relations between $\ln(K/K^b)$ and $1/T$ are shown in Fig. 8.

Figure 8 displays that $\ln(K/K^b)$ increases as the temperature decreases, and the remarkable linear

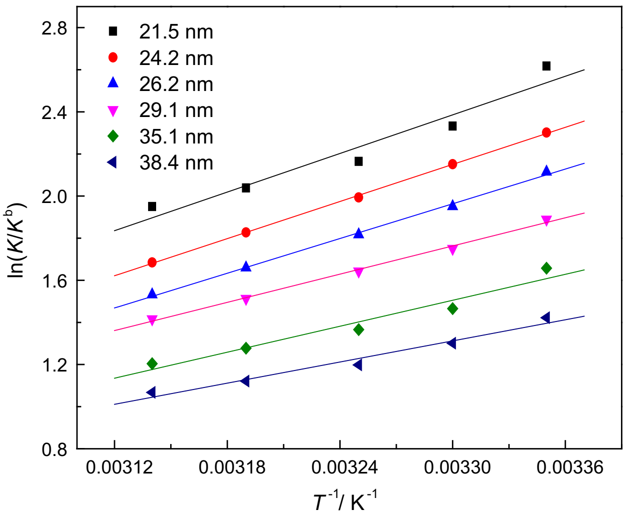

Figure 8 The relation between $\ln(K/K^b)$ and $1/T$.

trends verify the assumption that $\Delta_r H_m^s$ and $\Delta_r S_m^s$ can be regarded as constants in the temperature range of experiments. The molar surface enthalpy and entropy of nano-Cu can be calculated by Eq. (17) in combination with Fig. 8.

The relations between H_m^s and S_m^s, respectively, and $1/d$ are shown in Fig. 9.

As illustrated in Fig. 9, the particle size has a notable influence on H_m^s and S_m^s; the molar surface enthalpy and entropy increase with particle size decreasing and linearly vary with $1/d$, which agree with the theoretical analysis above. In addition, when the particle size tends to infinity, the molar surface enthalpy and entropy become zero.

Conclusions

For the influence regularities of nanoparticle size on the surface thermodynamic properties, the thermodynamic relations derived herein are consistent with the experimental results; with particle size decreasing, the molar surface Gibbs energy, the molar surface entropy and the molar surface enthalpy increase and linearly vary with the reciprocal of diameter for larger nanoparticles. Moreover, the ratio of the molar surface thermodynamic quantities to the corresponding partial molar surface thermodynamic quantities for spherical nanoparticles is 3:2. In addition, the surface tension decreases with increasing temperature and presents a linear variation with temperature. The new method proposed herein is capable of convenient and reliable determining the surface thermodynamic properties of nanoparticles to explain and predict the related thermodynamic behaviors involved in the preparations, researches and applications of nano-materials.

Acknowledgements

We are so grateful for the support from the National Natural Science Foundation of China (Nos. 21373147 and 21573157), which provides financial help in testing and characterization of the materials prepared.

Compliance with ethical standards

Conflict of interest The authors declare that they have no conflict of interest.

Figure 9 Relations of **a** H_m^s and **b** S_m^s with $1/d$.

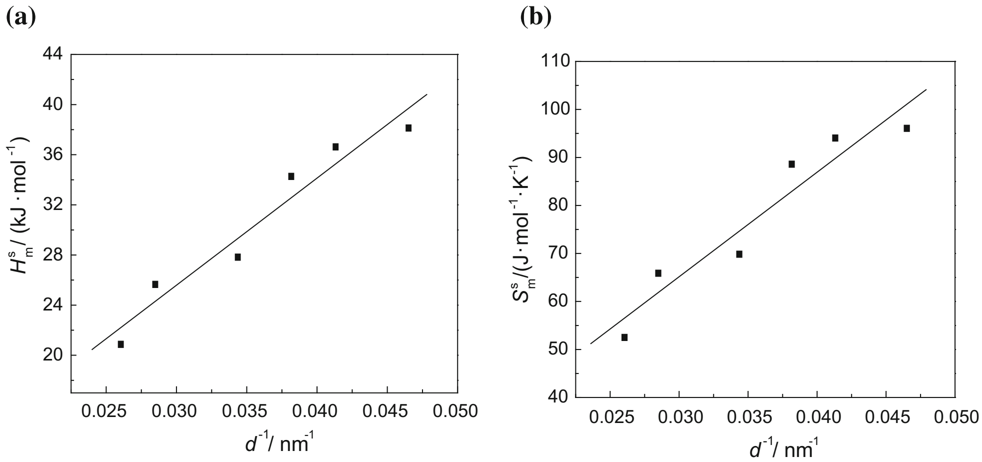

References

[1] Wen YZ, Xue YQ, Cui ZX, Wang Y (2015) Thermodynamics of nanoadsorption from solution: theoretical and experimental research. J Chem Thermodyn 80:112–118

[2] Cui ZX, Zhao MZ, Lai WP, Xue YQ (2011) Thermodynamics of size effect on phase transition temperatures of dispersed phases. J Phys Chem C 115:22796–22803

[3] Xue YQ, Zhao MZ, Lai WP (2013) Size-dependent phase transition temperatures of dispersed systems. Phys B Condens Matter 408:134–139

[4] Hiemstra T (2015) Formation, stability, and solubility of metal oxide nanoparticles: surface entropy, enthalpy, and free energy of ferrihydrite. Geochim Et Cosmochim Acta 158:179–198

[5] Vogelsberger W, Schmidt J (2010) Studies of the solubility of $BaSO_4$ nanoparticles in water: kinetic size effect, solubility product, and influence of microporosity. J Phys Chem C 115:1388–1397

[6] Mudunkotuwa IA, Rupasinghe T, Wu CM, Grassian VH (2012) Dissolution of ZnO nanoparticles at circumneutral pH: a study of size effects in the presence and absence of citric acid. Langmuir 28:396–403

[7] Zhang K, Han XP, Hu Z, Zhang XL, Tao ZL, Chen J (2014) ChemInform abstract: nanostructured Mn-based oxides for electrochemical energy storage and conversion. Chem Soc Rev 44:699–728

[8] Yang YF, Xue YQ, Cui ZX, Zhao MZ (2014) Effect of particle size on electrode potential and thermodynamics of nanoparticles electrode in theory and experiment. Electrochim Acta 136:565–571

[9] Okubo M, Hosono E, Kudo T, Zhou HS, Honma I (2009) Size effect on electrochemical property of nanocrystalline $LiCoO_2$ synthesized from rapid thermal annealing method. Solid State Ion 180:612–615

[10] Zhu JH, Fu QS, Xue YQ, Cui ZX (2016) Comparison of different models of melting transformation of nanoparticles. J Mater Sci 51:1–8. doi:10.1007/s10853-016-9758-1

[11] Yan AJ, Xue YQ, Cui ZX, Zhang Z, Wang SS (2016) Size-dependent dissolution kinetics of $CaCO_3$, nanoparticles in theory and experiment. J Mater Sci 52:1–9. doi:10.1007/s10853-016-0688-8

[12] Ball PA, Garwin L (1992) Science at the atomic scale. Nature 355:761–766

[13] Mazeina L, Deore S, Navrotsky A (2006) Energetics of bulk and nano-akaganeite, β-FeOOH: enthalpy of formation, surface enthalpy, and enthalpy of water adsorption. Chem Mater 18:1830–1838

[14] Bomatímiguel O, Mazeina L, Navrotsky A, Veintemillasverdaguer S (2008) Calorimetric study of maghemite nanoparticles synthesized by laser-induced pyrolysis. Chem Mater 20:591–598

[15] Li XX, Tang HF, Lu XR, Lin S, Shi LL, Huang ZY (2015) Reaction kinetic parameters and surface thermodynamic properties of Cu_2O nanocubes. Entropy 17:5437–5449

[16] Huang ZY, Li XX, Liu ZJ, He LM, Tan XC (2015) Morphology effect on the kinetic parameters and surface thermodynamic properties of Ag_3PO_4 micro-/nanocrystals. J Nanomater 2015:1–9

[17] Zhang Z, Fu QS, Xue YQ, Cui ZX, Wang SS (2016) Theoretical and experimental researches of size-dependent surface thermodynamic properties of nano-vaterite. J Phys Chem C 120:21652–21658

[18] Wang M, Zhu JH, Xue YQ, Cui ZX, Zhao MZ (2017) Size-dependent surface thermodynamic properties of silver oxide nanoparticles studied by electrochemical method. J Mater Sci 52:1039–1046

[19] Rekhviashvili SS, Kishtikova EV (2011) On the size dependence of the surface tension. Tech Phys 56:143–146

[20] Ono S, Kondo S (1960) Molecular theory of surface tension in liquids. Springer, Berlin, pp 134–280

[21] Sdobnyakov NY, Samsonov VM (2005) On the size dependence of surface tension in the temperature range from melting point to critical point. Cent Eur J Phys 3:247–257

[22] Samsonov VM, Bazulev AN, Sdobnyakov NY (2003) Surface tension in small droplets and nanocrystals. J Phys Chem 77:S158–S162

[23] Samsonov VM, Sdobnyakov NY, Bazulev AN (2004) Size dependence of the surface tension and the problem of Gibbs thermodynamics extension to nanosystems. Colloids Surf A 239:113–117

[24] Lu HM, Jiang Q (2005) Size-dependent surface tension and Tolman's length of droplets. Langmuir 21:779–781

[25] Xue YQ, Yang XC, Cui ZX, Lai WP (2011) The effect of microdroplet size on the surface tension and Tolman length. J Phys Chem B 115:109–112

[26] Zhang TY, Wang ZJ, Chan WK (2010) Eigenstress model for surface stress of solids. Phys Rev B 81:195427/1–195427/12

[27] Gao PP, Ma HX, Wu Q, Qiao LJ, Volinsky AA, Su YJ (2016) Size-dependent vacancy concentration in nickel, copper, gold, and platinum nanoparticles. J Phys Chem C 120:17613–17619

[28] Gao PP, Wu Q, Li X, Ma HX, Zhang H, Volinsky AA, Qiao LJ, Su YJ (2016) Size-dependent concentrations of thermal vacancies in solid films. Phys Chem Chem Phys 18:22661–22667

[29] Ma HX, Xiong XL, Gao PP, Li X, Yan Y, Volinsky AA, Su YJ (2016) Eigenstress model for electrochemistry of solid surfaces. Sci Rep 6:26897/1–26897/11

[30] Adamson AW, Gast AP (1997) Physical chemistry of surfaces, vol 48, 6th edn. Wiley, New York, pp 259–261

[31] Nanda KK (2005) Bulk cohesive energy and surface tension from the size-dependent evaporation study of nanoparticles. Appl Phys Lett 87:021909/1–021909/3

[32] Yaws CL (1999) Chemical properties handbook, 1st edn. McGraw-Hill, New York, pp 212–235

[33] Perry RH, Green DW (2008) Perry's chemical engineers' handbook, 8th edn. McGraw-Hill, New York, pp 2–136

[34] Xue YQ, Gao BJ, Gao JF (1997) The theory of thermodynamics for chemical reactions in dispersed heterogeneous systems. J Colloid Interface Sci 191:81–85

[35] Yang JG, Zhou YL, Okamoto T, Ryoichi I, Masazumi O (2007) A new method for preparing hydrophobic nano-copper powders. J Mater Sci 42:7638–7642

[36] Lubej A, Koloini T, Pohar C (1997) Solubility of copper(2) oxychloride. Ind Eng Chem Res 36:241–245